2009 International Nuclear Atlantic Conference - INAC 2009
Rio de Janeiro,RJ, Brazil, September27 to October 2, 2009
ASSOCIAÇÃO BRASILEIRA DE ENERGIA NUCLEAR - ABEN
***ISBN:* 978-85-99141-03-8**

STARTUP TRANSIENTS IN ACCELERATOR DRIVEN SYSTEMS USING CINESP-ADS CODE

Rubens Souza dos Santos [1,2]

[1] Instituto de Engenharia Nuclear (CNEN/IEN)
Rua Hélio de Almeida, 75 – Cidade Universitária – Ilha do Fundão – 21945-970
Rio de Janeiro - Brazil
rsantos@ien.gov.br

[2] Instituto Nacional de Ciência e Tecnologia de Reatores Nucleares Inovadores / CNPq

ABSTRACT

Accelerator Driven Systems (ADS) are subcritical nuclear reactor cores driven by spallation neutron source. These spallation neutrons are provided from the bombardment of a liquid metal flowing in a central region of the core, by a proton beam coming from a linear accelerator. Since neutron source dominates the neutronic of the ADS, its control usually is not related to the delayed neutron fractions as in the critical systems. In this way, ADS kinetics diverges from the former ones. This work presents some results of transients in ADS. Since ADS is to work in a pulsed regime, with time duration of pulse, a parametric result is showed to point out that different pulse durations should be studied in conjunction with pulse intensity, to maintain the ADS power stable. In addition, before generating these results, some transients were used to validate the CINESP-ADS code. It solves numerically the kinetic equations based on the multigroup diffusion theory, in One- or Two-dimensional, in the Cartesian or Cylindrical geometries, and for any energy and delayed neutron groups. Three-dimensional simulation is possible using a reactor transversal buckling. The numerical solution is obtained via finite differences for the spatial discretization, using the so-called box integration, and with the use of Alternating Direction Explicit (ADE) methods, for the time discretization. The code application to some transients due to source neutron variations demonstrates its efficiency and accuracy, when compared with analytical techniques, such as one that uses expansion in series of Helmholtz eigenfunctions.

Key Words: ADS, Reactor Kinetics, Multigroup Diffusion Theory, Numerical Methods

1. INTRODUCTION

Accelerator Driven Systems (ADS) are subcritical nuclear reactor cores driven by spallation neutron sources. Theses promising devices must be used not only as dedicated burners of transuranic elements but also as energy producers. Since the fuel materials to be used in these reactors must contain fertile-free fuels, it introduces some drawbacks in its operation. That derives from the fact that: most of these materials present low delayed neutron fraction; shorter neutron generation time than other reactor types; incipient Doppler Effect, among other things. In this way, the control of these systems is over the proton beam, which produces the source neutrons [1,2,3].

A Co-ordinated Research Project (CRP) on Analytical and Experimental Benchmark Analysis Driven System is ongoing, supported by IAEA [4]. This CRP aims to assist various national programs by providing collaborative research and development in the ADS technology, addressing all major physic phenomena of the spallation source and its coupling to the sub-critical system, such as YALINA-Booster in Belarus [5].

In this work we present numerical solutions for some transients of localized pulsed sources using CINESP-ADS computational code [6]. The objective is to qualify CINESP-ADS to be used for Yalina system in the scope CRP on Analytical and Experimental Benchmark Analysis Driven of the IAEA.

2. CINESP-ADS KINETIC MODEL

The physical model of the core reactor is dealt with considering the multigroup diffusion theory. To that we add the external neutrons source, allowing one- and two-dimensional calculations, in the Cartesian $(\alpha = 0)$ and Cylindrical $(\alpha = 1)$ geometries. With that we have [6]:

$$\frac{1}{\vartheta_g}\frac{\partial \varphi_g}{\partial t} = \frac{1}{x^\alpha}\frac{\partial}{\partial x}x^\alpha D_g \frac{\partial \varphi_g}{\partial x} + \beta\frac{\partial}{\partial y}D_g\frac{\partial \varphi_g}{\partial y} - D_g B_g^2 \varphi_g - \Sigma_{Rg}\,\varphi_g +$$

$$+\sum_{g'\neq g}^{G}\Sigma_{sg'g}\,\varphi_{g'} + \chi_{pg}(1-\beta)\sum_{g'=1}^{G}\nu_{g'}\,\Sigma_{fg'}\,\varphi_{g'} + \sum_{k=1}^{I}\chi_{agk}\lambda_k C_k + S_g\,, \quad g = 1,2,\ldots,G\,, \tag{1}$$

$$\frac{\partial C_k}{\partial t} = \beta_k \sum_{g'=1}^{G}\nu_{g'}\,\Sigma_{fg'}\,\varphi_{g'} - \lambda_k C_k\,,\ k = 1,2,\ldots,I\,, \tag{2}$$

where, $\varphi_g = \varphi_g(x,y,t)$, $C_k = C_k(x,y,t)$, and $S_g = S_g(x,y,t)$. For boundary conditions at bx and by we have:

$$\varphi_g(bx,by,t) = 0\,. \tag{3}$$

In case of $\alpha = 1$ we have:

$$D_g\frac{\partial \varphi_g(0,y,t)}{\partial x} = 0 \tag{4}$$

We point out here that the existence of the term $D_g B_g^2 \varphi_g$ in Eq. (1) permits to simulate until 3D problems.

3. NUMERICAL DISCRETIZATIONS

Equation (1) and (2) are discretized in space using the box integration, with mesh centered in the interface. The symbolic integrations are given by:

$$T_{gij}(t) = \int_{y_j-\frac{\Delta y}{2}}^{y_j+\frac{\Delta y}{2}} dy \int_{x_i-\frac{\Delta x}{2}}^{x_i+\frac{\Delta x}{2}} x^{\alpha} dx P_g(x,y,t) H_g(x,y,t) , \tag{5}$$

$$U_{kij}(t) = \int_{y_j-\frac{\Delta y}{2}}^{y_j+\frac{\Delta y}{2}} dy \int_{x_i-\frac{\Delta x}{2}}^{x_i+\frac{\Delta x}{2}} x^{\alpha} dx P_k(x,y,t) V_k(x,y,t) , \tag{6}$$

where $T_{gij}(t)$ and $U_{kij}(t)$ are generic terms, only time dependent, associated with the variables $H_g(x,y,t)$ and $V_k(x,y,t)$, respectively, as given in Eq. (1) and Eq.(2). When be the case, parameters $P_g = P_g(x,y,t)$ and $P_k = P_k(x,y,t)$ can represent mean properties, like Σ_{wg}, D_g etc., where w means the reaction types. The integrations given by Eq. (5) and Eq. (6) leads to the following matrix equation:

$$\frac{d\psi}{dt} = M\psi + S , \tag{7}$$

where $\psi = \psi(t)$ and $S = S(t)$ are vectors given by:

$$\psi(t) = col\{\varphi_{111}, \varphi_{121}, \ldots \varphi_{112}, \varphi_{122}, \ldots \varphi_{gij}, \ldots, \varphi_{GLN}, C_{111}, C_{121}, \ldots C_{112}, C_{122}, \ldots, C_{kij}, \ldots C_{ILN}\}, \tag{8}$$

$$S(t) = col\{S_{111}, S_{121}, \ldots S_{112}, S_{122}, \ldots S_{gij}, \ldots, S_{GLN}, 0,0,\ldots,0,\ldots,0,0\}, \tag{9}$$

and M is a matrix associated with the spatial discretizations of Eq. (1) and Eq. (2), which structure is shown in Fig. 1, considering: 2D, a grid of $L = 4$ and $N = 3$, two energy and one-precursor groups.

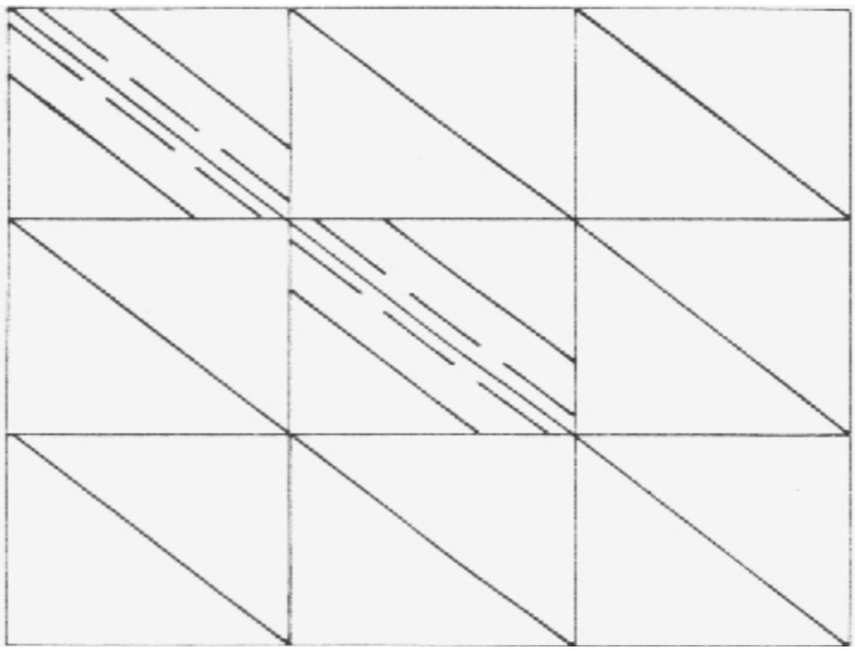

Figure 1. Block structures of matrix M.

Before discretizing Eq. (7) in time we use the fact of matrix M be able of splitting in such way:

$$M = D + E, \tag{10}$$

where matrices D and E have their structures given by Fig. 2 and Fig. 3.

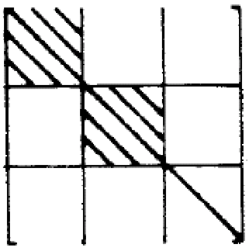

Figure 2. Structure of matrix D.

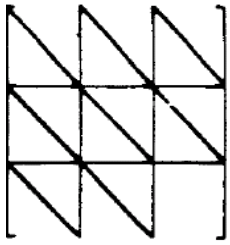

Figure 3. Structure of matrix E.

Now, using the ADE methods [7], the time derivative in Eq. (7) is approximated in two steps:

$$\frac{\psi^{n+1/2} - \psi^{n}}{\Delta t/2} \approx M_1\psi^{n+1/2} + M_2\psi^{n} + S^{n+1/2} + S^{n}, \tag{11}$$

$$\frac{\psi^{n+1} - \psi^{n+1/2}}{\Delta t/2} \approx M_3\psi^{n+1} + M_4\psi^{n+1/2} + S^{n+1} + S^{n+1/2}, \tag{12}$$

where, Δt is the time interval, $t_n = t_{n-1} + \Delta t$, and, $\psi^n = \psi(t_n)$. Matrices M_1, M_2 M_3 and M_4 are splitting of M, as the Alternating Direction Explicit Methods [6], given by Fig. 4 until Fig. 7.

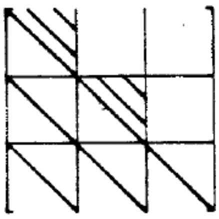

Figure 4. Structure of matrix M_1.

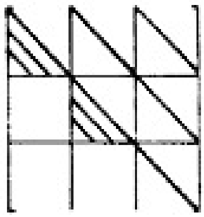

Figure 5. Structure of matrix M_2.

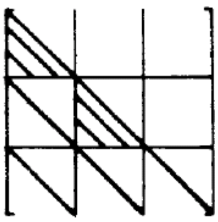

Figure 6. Structure of matrix M_3.

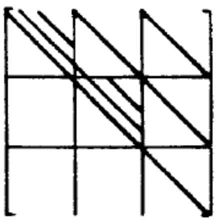

Figure 7. Structure of matrix M_4.

Defining I, in this context, as the identity matrix, Eq. (11) and Eq. (12) can be put in the following forms:

$$[2I - \Delta t M_1]\psi^{n+1/2} = [I + \Delta t M_2]\psi^n + \Delta t\left(S^{n+1/2} + S^n\right), \tag{13}$$

$$[2I - \Delta t M_3]\psi^{n+1} = [I + \Delta t M_4]\psi^{n+1/2} + \Delta t\left(S^{n+1} + S^{n+1/2}\right). \tag{14}$$

The right side of Eq. (13 and Eq. (14) are vectors, easily obtained by simple operations of multiplication. Fast algorithms can be improved, from matrix structures of the equations. That is possible because each block is dictated by the ordering given by Eq. (8). The spatial grid is marched in alternated directions, using Eq. (13) and Eq. (14). For each step, the equation system is solved simultaneously, in an explicit point wise way [6].

4. STEADY STATE CONDITION

The steady-state condition, considering the nominal condition, is obtained setting derivatives as zero, in Eq. (7). In this way, we have:

$$\psi(0) = M^{-1}S(0), \tag{15}$$

As M is a sparse matrix, the iterative method Successive Over-Relaxation is used to obtain $\psi(0)$ [8]. Indeed, as external source neutron it is which sets neutron fluxes, first all, a subcritical core is searched, for a given $\kappa_{eff} < 1$. Done that, the nominal power is defined using the following equation:

$$P(0) = \sum_{g=1}^{G} \iint dxdy \Sigma_{fg}(x, y, 0)\varphi_g(x, y, 0). \tag{16}$$

5. RESULTS

5.1. CINESP-ADS Validation

First of all, CINESP-ADS was validated using data for a 1D uniform slab, from reference [9]. Table I and Table II show multigroup constants, considering 3 energy groups. With that, a search of sub criticality was made in order to find a state where $K_{eff} = 0.9858184$, which implied a slab of 23.064cm. In this calculation, $\Sigma_{s1\rightarrow 3} = 0$ because the version of CINESP for criticality search was developed for direct coupling for scattering cross-sections, $\Sigma_{sg-1\rightarrow g}$.

Table I. Group parameters.

g	1	2	3
$\vartheta_g\,(cm/s)$	1.866x10^7	6.768x10^6	7.501x10^5
χ_{pg}	0.7112	0.2886	2.0x10^{-4}
$\Sigma_{ag}\,(cm^{-1})$	0.01403	0.01638	0.06985
$\upsilon\Sigma_{fg}\,(cm^{-1})$	0.03453	0.03287	0.12
$D_g\,(cm)$	1.177	0.9123	0.509
$S_g\,(n/s.cm^3)$	1.	0.0	0.0

Table II. Group scattering cross-sections.

g	1	2
$\Sigma_{g\rightarrow g+1}\,(cm^{-1})$	3.318x10^{-2}	3.45x10^{-4}
$\Sigma_{g\rightarrow g+2}\,(cm^{-1})$	1.166x10^{-5}	

Fig. (8) shows the slab with its source location. Throughout applications was used a spatial grid with 39 meshes and one very low delayed neutron fraction $(\beta \approx 0)$. Also, spallation neutrons were considered all being born in-group 1 $(S_2 = S_3 = 0)$. Target is located at region II, but I, II and III ones, have the same properties.

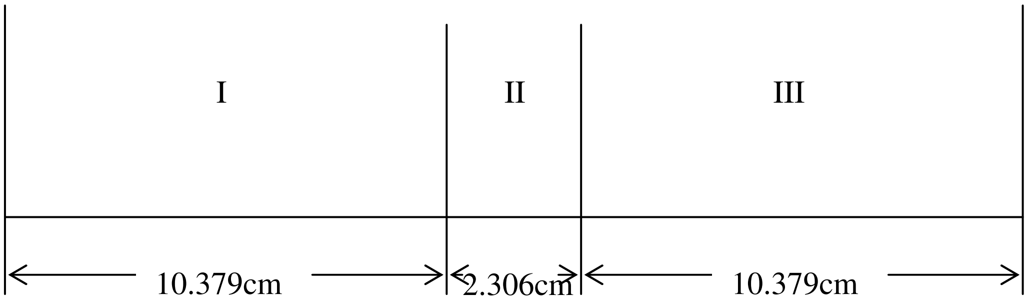

Figure 8. Slab dimensions and source location.

Fig. (9) exhibits the normalized flux distribution in the slab.

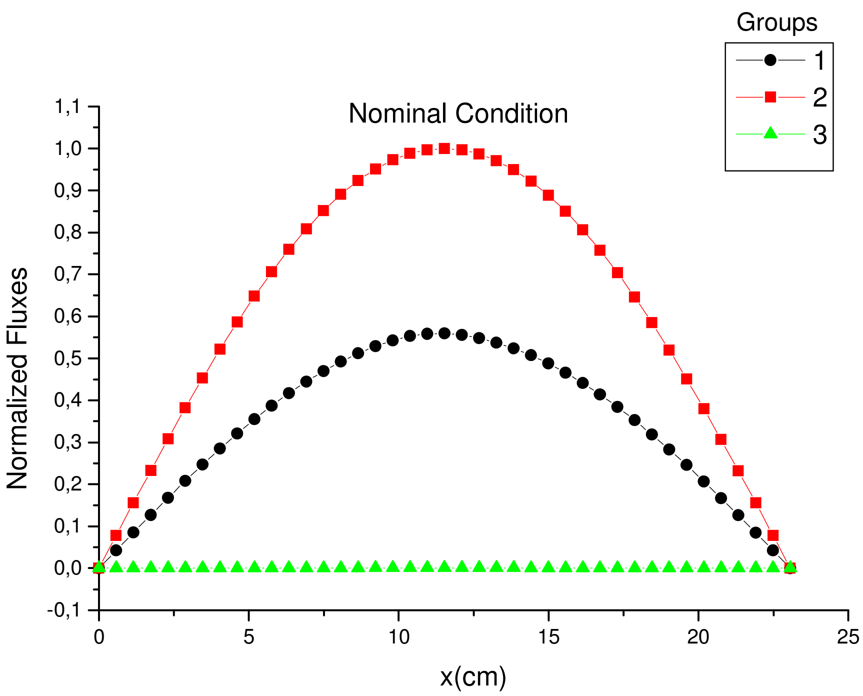

Figure 9. Flux distribution.

CINESP-ADS solution was compared with an analytical approach, based on Helmholtz eigenfunctions, disregarding delayed neutrons [9]. For that, use was made of 150 harmonics to reduce the error due to the series truncation. The transient starts with zero flux, when a pulse of $10\mu s$ duration and intensity $S_1 = 1$ $(S_2 = S_3 = 0)$. After that the system was shuts down. Fig. 10 and Fig 11 show power variation, based on CINESP-ADS and analytical solutions. Fig. 12 and Fig. 13 exhibits variations between 5 and $25\mu s$. We can note good agreement between CNESP_ADS and analytical solution.

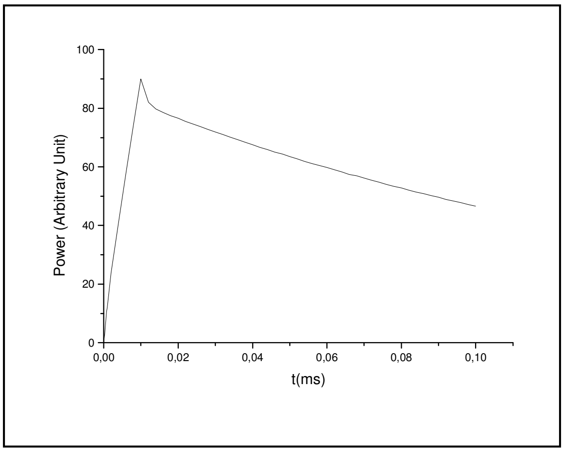

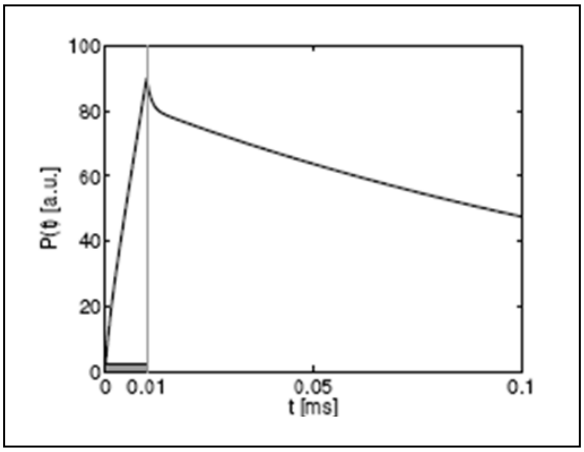

Figure 10. CNESP-ADS solution - 1 pulse.

Figure 11. Analytical solution - 1 pulse.

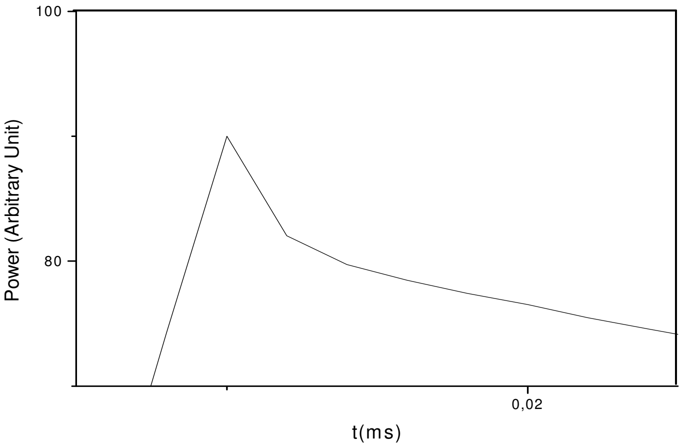

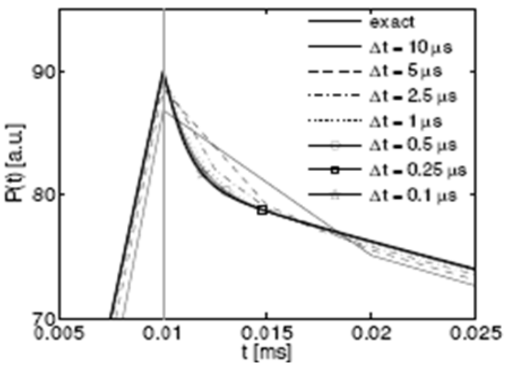

Figure 12. Zoom: CNESP-ADS solution.

Figure 13. Zoom: Analytical solution.

5.2. Power transient

CINESP-ADS was applied to calculate a power transient, simulating a power elevation, followed a shutdown. The transient is defined by: $S_1(0) = 1$; during $\tau_1 = 10\mu s$, $S_1(t) = 5$; after $t > 10\mu s$, $S_1(t) = 0$. In this transient, the time-step was $\Delta t = 10^{-7} s$. The grid was the same above. The duration of the transient was $100\mu s$. Fig. 14 shows CINESP-ADS and Analytical solution [10], where we can see the excellent agreement between the methods. Once more CINESP-ADS was validated. Fig. 15 shows the normalized flux variations.

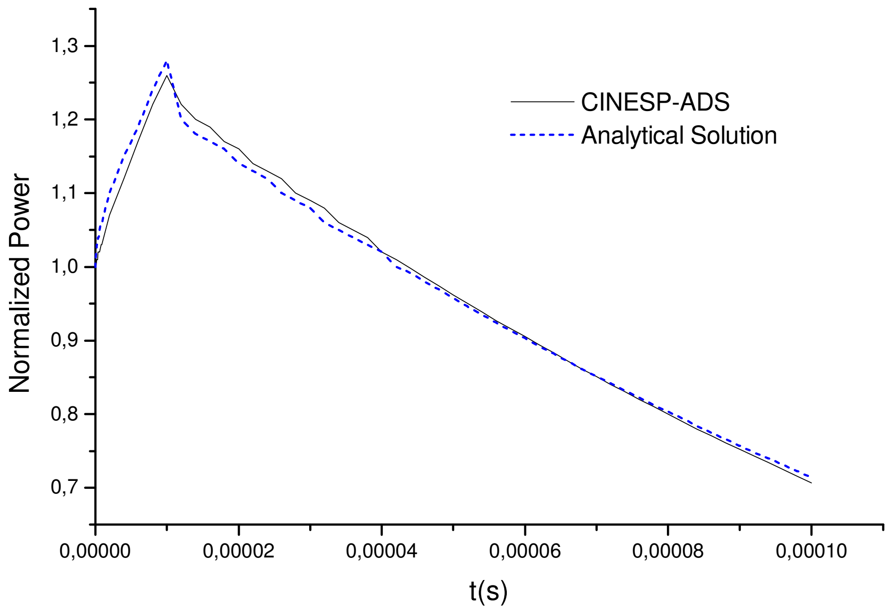

Figure 14: Normalized power variation.

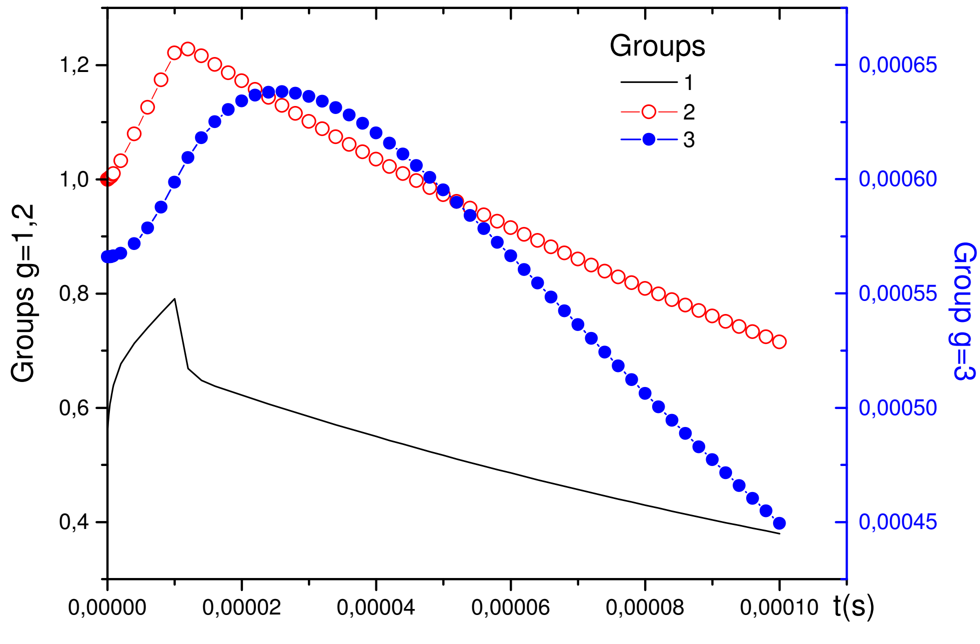

Figure 15. Normalized flux variation.

5.3. Startup transient

The startup transient consists in bringing the ADS from zero power to nominal power. For that, a pulse train initiates the transient. Each pulse has a duration time $\tau_1 = 25\mu s$ and the same time of turn off, $\tau_0 = 25\mu s$, representing a period $T = \tau_0 + \tau_1 = 50\mu s$. The startup is observed during $60s$, using a time-step $\Delta t = 12.5 \mu s$. The source intensity was setup as $S_1 = 2$ ($S_2 = S_3 = 0$). The intensity 2 is necessary because half of transient the source is turned off. Step transients were also calculated in order to compare the asymptotic behavior. In this case, the source intensity was set as 1, obviously. Fig 16 shows the normalized power for both transients.

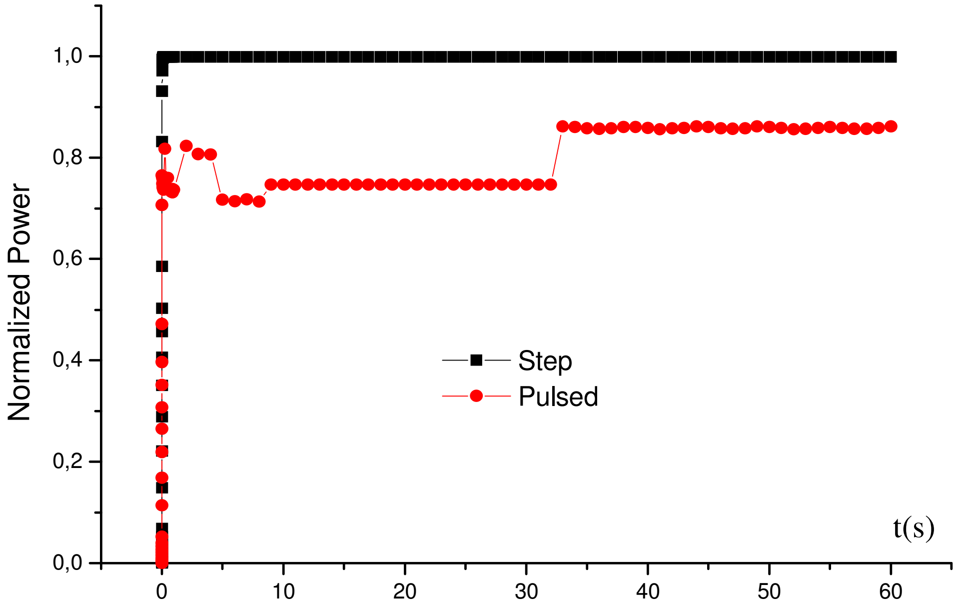

Figure 16. Power due to source variation in step and pulses.

5.4. Pulse duration effects

Fig. 17 shows the differences due to the pulse duration. We can see that the ADS proton beam bunches must be synchronized with the beam intensity to maintain the ADS power stabilized.

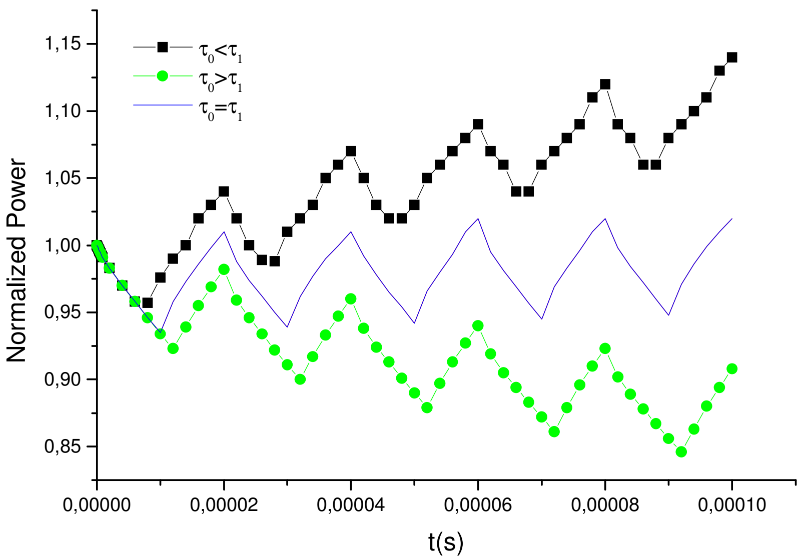

Figure 17. Pulse duration effects on the power.

3. CONCLUSIONS

Two important transients were calculated using CINESP-ADS. In both was demonstrated the necessity to observe the ADS operation since the startup. The frequency of pulses plays an important role in the modulation of the intensity. Before these analyses, in addition, comparing numerical results with analytical ones, we were able of validating CINESP-ADS. The application of Code to pulsed source transient showed that it is able to provide consistent results of a step source. Even though, the application was circumspect to one-dimensional problems, CNESP-ADS can be applied to analysis the Benchmark problem proposed for YALINA-Booster, a typical Three-dimensional problem in Cartesian geometry.

ACKNOWLEDGMENTS

The author would like to thank the National Council for Scientific and Technological Development (CNPq) of Brazil, for the financial support.

REFERENCES

1. C. Rubbia et al, Conceptual Design of a Fast Neutron Operated High Power Energy Amplifier, *CERN/AT/95-44 (ET*), 29th September (1995).
2. M., Eriksson, J.E., Cahalan, W.S., Yang, On the Performance of Point Kinetics for the Analysis Accelerator-driven Systems, *Nuclear Science and Engineering*, **149**, 298-311 (2005).
3. H. A. Abderrahim et al, MYRRHA: A multipurpose accelerator driven system for research & development, *Nuclear Instruments and Methods in Physics Research A 463*,487-994, (2001).
4. H.A., Abderrahim, A., Stanculescu, IAEA Coordinated Research Project on Analytical and Experimental Benchmark Analyses of Accelerator Driven Systems, *Proceedings of ANS Topical Meeting on Reactor Physics, PHYSOR 2006*, Vancouver, (2006).
5. V., Bournos, C., Routkovskaia, I., Serafimovich, H.I., Kiyavitskaya, Yu., Fokov, A., Fokov, S., Mazanik, A., Adamovich, T., Korbut, A., Koulikovskaya, A., Khilmanovich, B., Martsinkevich, S., Chigrinov, Experimental Investigations on ADS at Sub-Critical Facilities of Joint Institute for Power and Nuclear Research-Sosny of the National Academy of Sciences of Belarus, *Meeting of the CRP Analytical and Experimental Benchmark Analyses of Accelerator Driven Systems*, Minsk, 5-9 December (2005).
6. R.S., Santos, Dynamics of Nuclear Core Based on One- and Two-dimensional Multigroup Diffusion Theory, *X ENFIR*, (1995).
7. Wm.H., Reed and K.F., Hansen, Alternating Direction Methods for the Reactor Kinetics Equations, Nucl. Sci, Eng., **41**, 431, (1970).
8. M., Clark Jr. and K.F., Hansen, Numerical Methods of Reactor Analysis, *Academic Press Inc.*, New York, (1964).
9. S., Dulla, P., Ravetto, P., Picca, D., Tomatis, J.R., Maiorino, T., Carluccio, A., Antunes, A., Santos, F., Oliveira, R.S., Santos, Analytical Benchmarks for the Kinetics of Accelerator-Driven Systems, *Joint International Topical Meeting on Mathematics & Computation and Supercomputing in Nuclear Applications (M&C+SNA 2007)*, Monterrey, California, (2007).
10. F.L., Oliveira, Solução Analítica da Cinética Espacial do Modelo de Difusão para Sistemas Homogêneos Subcríticos Acionados por Fonte Externa, *Master Thesis - IPEN-USP*, SP, Brazil, (2008).